Application of Chaos Analysis to Electrostatic Measurements of Horizontal Gas-solid Flow in Pneumatic Conveying of Plastic Pellets

Osamh S. Alshahed, Baldeep Kaur, and Michael S.A. Bradley

The Wolfson Centre for Bulk Solids Handling Technology, University of Greenwich, Central Avenue, Chatham Maritime, Kent, ME4 4TB, United Kingdom

ABSTRACT Chaotic invariant measures have been used to characterise the instabilities of fully developed gas-solid flow patterns in horizontal pneumatic conveying of plastic pellets. These measures were applied to phase spaces (attractors) reconstructed from bottom arc-shaped electrostatic signals to characterise the behaviour of flow patterns: stratified flow, pulsating flow, moving dunes and blowing dunes. The flow patterns were identified using high-speed video imaging sight section of a pipeline and classified at several operating conditions in a flow pattern map and state diagram. It is found that optimal operating conditions at the minimum conveying air velocity in the state diagram are between moving dunes and blowing dunes. Chaotic features of electrostatic phase spaces are characterised using statistical measures capable of staying invariant at specific operating conditions, including Lyapunov exponent, approximate entropy and correlation dimension. The correlation between the chaotic invariant measures with the operating conditions is analysed through state diagrams, indicating that the fluctuations of electrostatic signals can classify the flow patterns at different solid mass flow rates.

1. INTRODUCTION

Dilute phase, transition phase and dense phase flows are the main modes of operation in a pneumatic conveying system. The flow pattern map and the state diagram are common ways of describing the gas-solid flow transition spectrum from dilute to dense phase flow operations for specific particulate material. The flow pattern map shows distributions of operating parameters, including air and solids mass flow rates, classified according to the observed flow patterns in a transparent pipeline [1], [2]. The state diagram is a function that relates average air velocity with air pressure drop per unit length of a pipeline having a constant inner diameter [1], [3]. The pressure drop directly relates to the air velocity in dilute phase flow operation and shifts to an indirect relationship for dense phase flow. The air velocity at the centre of this shifting curve is the optimal pneumatic conveying condition for minimum energy consumption, known as minimum conveying air velocity (MCAV). While the pressure drop line connecting the MCAV at different solid mass flow rates is known as the pressure drop minimum curve (PMC).

The instabilities of flow patterns in the transition phase from dilute to dense phase flow increase as the operating conditions approach the PMC. The flow patterns in the transition phase near the PMC are rich with complex nonlinear dynamics. These dynamics can quantitatively be explored using high-dimensional phase spaces (attractors) reconstructed from time-series state measurements using the time-delay coordinate embedding method [4]. A phase space reconstructed from one state measurement of a system can reveal equivalent topology to the system state space. The topological feature of a reconstructed phase space can be described using statistical measures that, if captured correctly, can stay invariant across similar future phase space topologies, including fractal dimension, largest Lyapunov exponent (LE) and entropy [5]. The chaotic behaviour of an attractor is quantified using the LE measure, reflecting the separation of neighbouring trajectories in each dimension of the attractor.

Considerable efforts have been made to characterise the complex dynamics of gas-solid flow patterns in horizontal pneumatic conveying systems through visual observation of 2D and 3D phase space reconstructed from pressure time-series signals [6]–[8]. Moreover, phase space invariant measures of gas-solid flow have been extensively studied in fluidised bed systems [9]–[13]. However, few studies aim to quantify the complex dynamics of gas-solid flow in pneumatic conveying systems [6], [14]. The fractal dimension of the gas-solid flow pattern was studied by [6] using the Hurst exponent developed from pressure sensor signals in a horizontal pneumatic conveying system, indicating that the dilute phase has higher fractal complexity than the dense phase. Fu *et al.* [14] characterised gas-solid flow dynamics in a vertical pneumatic conveying system of fine pulverised coal using the approximate entropy measure from electrostatic signals as a measure of solid concentration to distinguish dilute

from dense phase flow operations. It is found that the approximate entropy of electrostatic signals is higher in the dense phase than in the dilute phase flow operation.

This paper aims to develop the LE measures from bottom arc-shaped electrostatic sensor time series data to characterise the chaotic behaviour of gas-solid flow in a horizontal pipeline system. The LE measure is calculated from a moving window of time-series data with a fixed step, allowing the flow complexity to be monitored in real time near the MCAV. The parameters set for developing the LE measure are estimated using a heuristic procedure or set to a constant.

2. EXPERIMENTAL SETUP

Experimental tests have been conducted in a close-loop industrial-scale pneumatic conveying system to capture fully developed gas-solid flow behaviour in a horizontal pipeline. Figure 1 shows a schematic of the industrial-scale pneumatic conveying system and its main components. The main components of the pneumatic conveying system consist of a 0.1 m inner diameter pipeline with a total length of 127 m, receiving hopper and blow tank with a 1.5 m^3, a screw feeder, and a nozzle bank. In the loop, there are eight bends and two vertical pipeline sections. The loop consists of horizontal pipeline sections except for the sections before the second bend and after the last bend. Two screw-type compressors are used to compress air in tanks at 5.2 bar, which is then regulated and introduced in the pipeline cycle from the blow tank to receiving hopper using the nozzle bank at two locations: the blow tank exit, also known as 'blow tank air' (the screw feeder inlet), and the pipeline inlet also known as 'supplementary air' (the screw feeder outlet). The blow tank and supplementary air ratio can be adjusted per the requirement. Particulate materials are first fed to the blow tank through the feed hopper, then the blow tank is pressurised, and material is fed to the pipeline through a screw feeder using the blow tank and supplementary airflow. The air is separated from solids at the receiving hopper through a bag filter house with a surface area of 35 m^2.

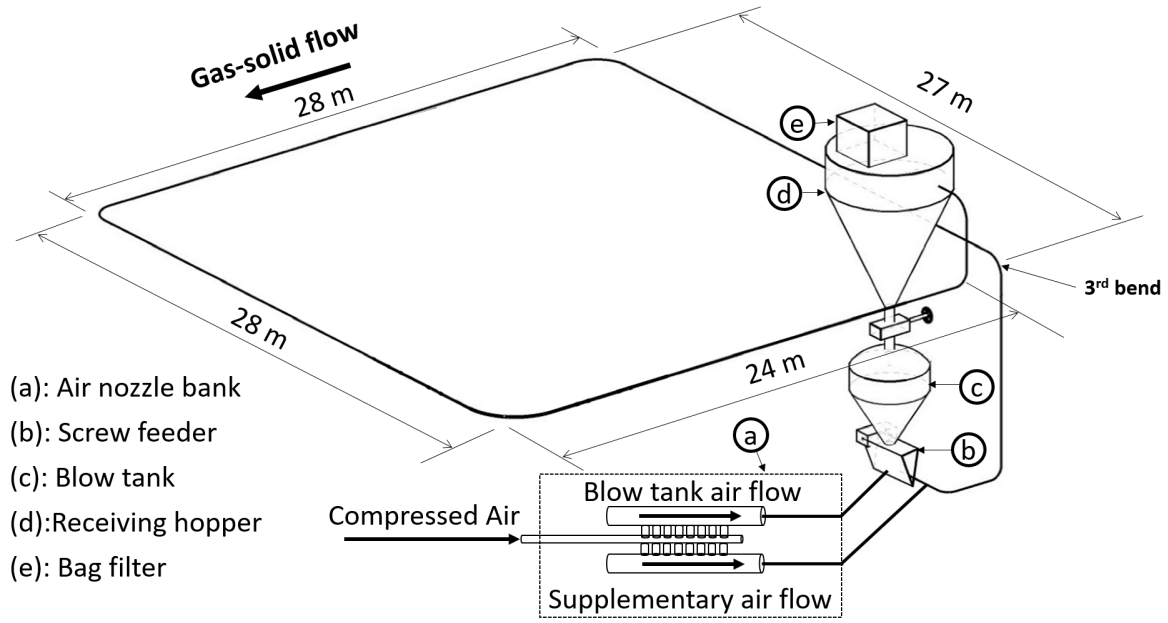

Figure 1 A schematic of the pneumatic conveying system set-up used to study the fully developed gas-solid flows in the horizontal pipeline downstream of the third bend

The solid mass flow rate is measured using a load cell at the receiving hopper and controlled by choosing a suitable air ratio between the blow tank and supplementary air and screw feeder motor speed. The air mass flow rate at the inlet of the pneumatic conveying pipeline system is controlled using the nozzle bank. The nozzle bank consists of two sets of eight nozzle sizes, which can incrementally control the air mass flow rate at the blow tank exit and pipeline inlet using different combinations of nozzles for each set, each with a maximum limit of 0.38 kg/s.

Pressure measurements of gas-solid flow are undertaken using eight pressure transducers manufactured by DRUCK, with measurements ranging from 0 to 40kPa. Pressure sensors are installed 8 m downstream of the third

bend to ensure gas-solid flow is transitioned from accelerating to fully developed. The first set of four pressure sensors is installed equidistantly with a 2m separation distance, while the second set of four pressure is installed 4m after the fourth sensor with an equidistance of 2m. Kumar *et al.* [15] developed the top and bottom arc-shaped electrostatic sensors assembly to measure the average velocity of charged particles. The primary source of electrostatic charge carried around solid particles is the collisional friction between particles and the surrounding pipeline inner wall, which continuously goes through positive and negative charges with a bimodal distribution. If fully charged particles pass through the 100% sensitivity zone (bottom section of the pipeline cross-section), the voltage signal will have high magnitudes and then return to zero and vice versa. The arc-shaped electrostatic sensors assembly is placed at 0.62 m from the first pressure sensor (P1), followed by a transparent pipeline to capture flow patterns using a high-speed video camera capturing images at 240 fps, as shown in Figure 2.

Electrostatic signals were acquired from the bottom arc-shaped electrostatic electrode, which is amplified first using a transimpedance amplifier circuit with a measurement range from -5 to +5 volts and then sampled with the first pressure sensor (P1) using the National Instrument USB 6211 module at a frequency of 525 Hz. The Load cell and the rest of the pressure sensors from P2 to P8 are sampled at 1 Hz using National Instrument 6208, which is sufficient for state diagram representation. LabVIEW software is used to acquire data from the National Instrument modules, while the data analysis calculations are developed in MATLAB software.

A 2D grid of operating parameters is considered, including solids mass flow rate and air mass flow rate, to study gas-solid flow patterns behaviour of plastic pellets and their effect on pressure signal and bottom arc-shaped electrostatic signal. Cubical shape plastic pellets with a total batch mass of 800 kg are used, having a mean diameter of 3.6 mm, particle density of 910 kg/m^3 and bulk density of 560 kg/m^3. The air mass flow rate injected into the blow tank was kept constant throughout the transport process, and the screw feeder speed was set to five different incremental values. The solids mass flow rate is calculated using a linear regression fit of the measured solid mass time-series signal in the fully developed flow region. The average pressure values from pressure sensors P1 to P8 are used to calculate the average pressure drop through a single regression fit across the eight sensors.

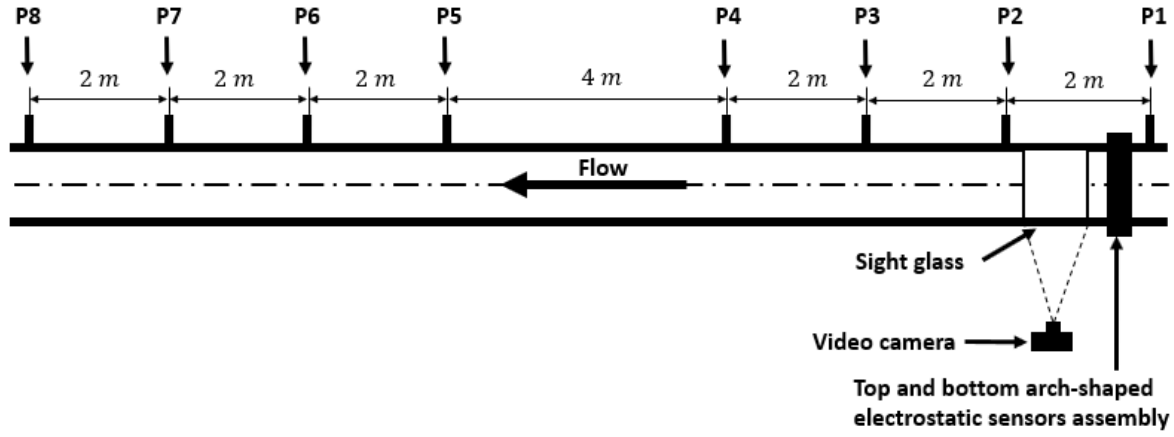

Figure 2 A schematic diagram of the horizontal pipeline downstream of the third bend showing 8 pressure sensors location from P1 to P8 and the top and bottom arc-shapes electrostatic sensors assembly.

The initial experimental test point at constant screw feeder speed was conducted at a high supplementary air mass flow rate (0.4 kg/s) at the inlet of the transport pipeline to transport plastic pellets through dilute phase flow operation. Then the following test points were measured at the same screw feeder speed, and the supplementary air mass flow rate was progressively decreased by 0.02 kg/s using the nozzle bank until a single slug flow or settled layer appeared in the transparent pipeline. According to plug flow type capable materials, unstable flow in the form of slugs exists at an air velocity below the MCAV [1]. Therefore, further experiments are conducted at a constant solids mass flow rate and progressively decreasing the air mass flow rate for each test to ensure that the transition flow spectrum between dilute and dense phase flow is captured using the installed sensors to identify the MCAV.

3. ANALYSIS METHOD

3.1 Phase Space

Time-delay coordinate embedding is used to reinflate a state variable from time-series measurements into a vector of latent state variables under the assumption that the underlying dynamic is smooth with low-dimensional manifolds [4]. This method reconstructs a high dimensional phase space from a time-series signal that, if captured correctly, can have topological equivalence to the original system state space. Reconstructing a phase space using the time-delay coordinate embedding from measurements requires two main parameters - time delay and embedding dimension. Consider a signal $X(t) = (x(t_1) \dots x(t_n))$, where n is the number of points acquired at constant sampling periods. Equation 1 shows the phase space data is in the form of a vector $Y(t)$ represented in the matrix form, where m is the embedding dimension, τ is the time delay, and N is the number of points in phase space ($N = n - (m-1)\tau$).

$$Y(t) = \begin{bmatrix} x(t_1) & x(t_{1+\tau}) & x(t_{1+2\tau}) & \cdots & x(t_{1+(m-1)\tau}) \\ x(t_2) & x(t_{2+\tau}) & x(t_{2+2\tau}) & \cdots & x(t_{2+(m-1)\tau}) \\ \vdots & \vdots & \vdots & \ddots & \vdots \\ x(t_N) & x(t_{N+\tau}) & x(t_{N+2\tau}) & \cdots & x(t_{N+(m-1)\tau}) \end{bmatrix} \quad (1)$$

When the dynamic complexity in a time series signal is generated from a stochastic dynamical system, its reconstructed attractor will correspond to infinite-dimensional space with no meaningful information. The false nearest neighbour Algorithm (FNN) is a commonly used algorithm to estimate the embedding dimension of a signal, which is based on the idea that if not enough dimension is used to unfold the dynamics, there will be trajectory crossings in the dynamics [16]. These crossings are noise caused by high to low-dimensional space projection. This algorithm scans for trajectory crossings by distinguishing true neighbouring points from false ones for an attractor while increasing the embedding dimension. The recommended heuristic for FNN parameters is to select an embedding dimension that satisfies 10% of false neighbours, determined at a distance threshold 1.

3.2 Largest Lyapunov Exponent

The sensitivity of initial conditions is a natural phenomenon that describes chaotic behaviour, quantified using the Lyapunov exponent. Lyapunov exponent characterises the separation rate between two neighbouring trajectories in phase space. There are as many Lyapunov exponents across time as there are dimensions known as the Lyapunov spectrum, which correspond to each separation direction in phase space. If all the Lyapunov exponents of an attractor are negative, all trajectories are shrinking from all directions towards stable manifolds. If all Lyapunov exponents are positive, then trajectories diverge in unstable manifolds. To have an attractor means the sum of all Lyapunov exponents tends to approach zero and negative for dissipative systems. For a chaotic attractor, there is at least one positive Lyapunov exponent. However, this cannot indicate whether an attractor is chaotic, as there will be a combination of stable and unstable manifolds. Typically, the positive Lyapunov exponent in a set of initial conditions dominates growth in an attractor in the long run.

In this study, only the largest Lyapunov exponents (LE) are used to measure chaotic behaviour in phase space. The algorithm for the LE is adopted from Rosenstein [17]. Lyapunov exponent $\lambda(i)$ is a function of phase point i across the expansion step k, presented in Equation 2. The value of k_{min} and k_{max} are the minimum and maximum values of the expansion range. Where $\|Y_i - Y_s\|$ is the distance between each phase point i and its nearest neighbour s and $\|Y_{i+k} - Y_{s+k}\|$ is the change after an expansion step k. The nearest neighbour points in this algorithm satisfy the condition $|\mathrm{i} - \mathrm{s}| > minimum\ separation$. The minimum separation is calculated using the ratio of the sampling frequency of the signal to its mean frequency, allowing enough space for initial conditions from neighbouring trajectories of interest to be considered. For each expansion step, one value of the Lyapunov exponent is calculated using the average of positive Lyapunov exponents for all the phase points, also called average log divergence (ALDiv). Across the expansion steps from k_{min} and k_{max}, a single value for the Lyapunov exponent is calculated through linear regression fit across an expansion range of interest. A phase space with positive LE indicates that the dominant structure is chaotic, negative LE indicates dissipative nature, and zero LE represents periodic or fixed points.

$$\lambda(i) = \frac{1}{k_{max} - k_{min} + 1} \sum_{k=k_{min}}^{k_{max}} \frac{1}{k \times dt} ln \frac{\|Y_{i+k} - Y_{s+k}\|}{\|Y_i - Y_s\|} \quad (2)$$

4. RESULTS AND DISCUSSIONS

4.1 Flow Pattern Map and State Diagram

The flow pattern map illustrates the formation of gas-solid flow patterns at different operating conditions. It is a scatter of operating points, including solids mass flow rate and air mass flow rate, classified into regions identified based on the flow pattern observed in a transparent pipeline. Tsuji studied the wall pressure fluctuation of horizontal gas-solid flows of plastic pellets with a mean diameter of 2.3 mm and observed its flow patterns close to the PMC, describing them as sliding dense clusters [19]. Cabrejos provided more generalised descriptions of horizontal gas-solid flow patterns and their relations to the operating conditions using three materials with different material properties [6]. The flow patterns identified for plastic pellets with a mean diameter of 3 mm are homogenous flow, stratified flow, pulsating flow, moving dunes and blowing dunes. Figure 3 shows the flow pattern map for horizontal pneumatic conveying of plastic pellets with a mean diameter of 3 mm classified into three patterns: stratified/pulsating flow, moving dunes and blowing dunes. The regions of these flow patterns vary across different gas and solids mass flow rates. Beyond the left boundary, slug flow (region D) and settled layer (region E) are present in the upper and lower regions.

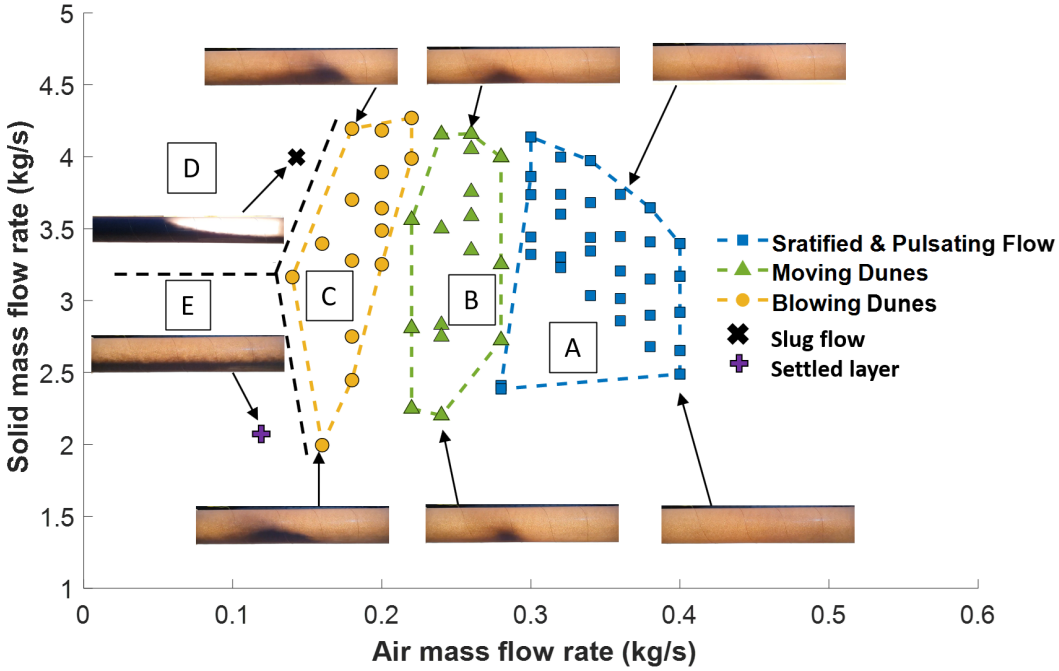

Figure 3 The flow pattern map for horizontal pneumatic conveying of plastic pellets

At a high air mass flow rate of 0.4 kg/s and low solids mass flow rate of 2.48 kg/s (lower boundary of region A), plastic pellets are in suspension mode, where particles are distributed across the pipeline cross-section with high solids concentration at the lower section of the pipeline, namely stratified flow. At the same air mass flow rate but higher solids mass flow rate of 3.6 kg/s (lower to the upper boundary in region A), plastic pellets are in an intense kinetic and frictional collision as they accumulate and form discontinuous clouds at the bottom of the pipeline, known as pulsating flow. As the air mass flow rate reduces (transition from region A to B) at a particular point, which is 0.28 kg/s in this case, self-organised critical states appear as moving dunes surrounded by dilute phase sliding on the bottom of the pipe. Moving dunes are featured by continuous erosion at the up-wind side (luff) and deposition at the down-wind side (lee). With further reduction in air mass flow rate, solid particles in dilute phase flow start to drop out of suspension, and multiple moving dunes slow down and merge, forming blowing dunes. At the left boundary of blowing dunes, dunes start to settle down, and the transportation mechanism starts to be dominated by saltation and surface creep. Beyond this boundary, plug flow (region (E)) and settled layer (region (D)) at the upper and lower regions are present.

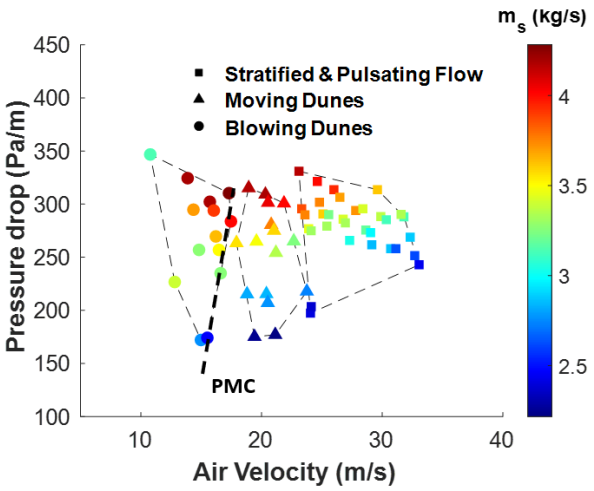

Figure 4 State diagram of plastic pellets with classified flow patterns regions

Coarse solid particles like plastic pellets with a mean diameter greater than 1 mm are expected to be conveyed at the MCAV without blockages [18]. Figure 4 shows a state diagram developed using the data gathered from the horizontal pneumatic conveying of the plastic pellets with a mean diameter of 3.6 mm. The operating points considered in developing the state diagram are the same as in the flow-pattern map presented in Figure 3. Each solid flow rate value is included for each point through a colour spectrum referring to the colour bar of values, and the flow patterns are classified into regions. The superficial air velocity is calculated based on the mean pressure and pipe diameter using the ideal gas law at ambient temperature and plotted as a function of the pressure drop per unit length of pipe. Correlating the superficial air velocity and pipeline pressure drop with gas-solid flow patterns show how specific flow patterns influence the pressure drop. The superficial air velocity in stratified, pulsating and moving dunes directly relates to the pressure drop. While the superficial air velocity of blowing dunes has an indirect relationship with the pressure drop, indicating that the PMC is between moving dunes and blowing dunes.

4.2 Chaotic Analysis of Electrostatic Sensor Data

The Lyapunov exponent analysis is applied to a moving time window of the bottom arc-shaped electrostatic sensor data to monitor the change in the chaotic behaviour of the flow at different operating conditions. The parameters required to calculate the largest Lyapunov exponent (LE) as a time series are moving window size and step, embedding dimension and time delay to reconstruct phase spaces and maximum expansion step (K_{Max}) to compute slopes of the average log divergence (ALDiv).

The moving window size is set to 5s of data (2625 data points) and the window step to 2.5s (1312 data points). The phase spaces are reconstructed using a time delay of 1, and the embedding dimension is estimated using FNN. The embedding dimensions are estimated for the electrostatic sensor data acquired at the operating points in Figure 3, which vary between 9 and 13. The choice of dimension used to reconstruct the moving phase spaces window is 10. Calculating a single LE requires linear regression across an expansion range k in the ALDiv function.

Figure 5(a) presents ALDiv as a function of an incremental expansion time step (k) for a 5s phase space window. The initial trends of ALDiv are a linear increase reflecting chaotic behaviour (positive LE). The trend then shifts to a relatively constant value at k = 10. This shift consistently occurs at k = 10 across the 30s of electrostatic sensor data at the operating points in Figure 3. The K_{Max} used to estimate LE for the moving window is 10 steps across all operating conditions. Figure 5(b) shows LE time-series signals developed from electrostatic sensor data acquired at three different air velocities higher, at and below the MCAV 33, 20 and 10 m/s, indicating an increase in LE value as the flow transition from stratified flow to blowing dunes.

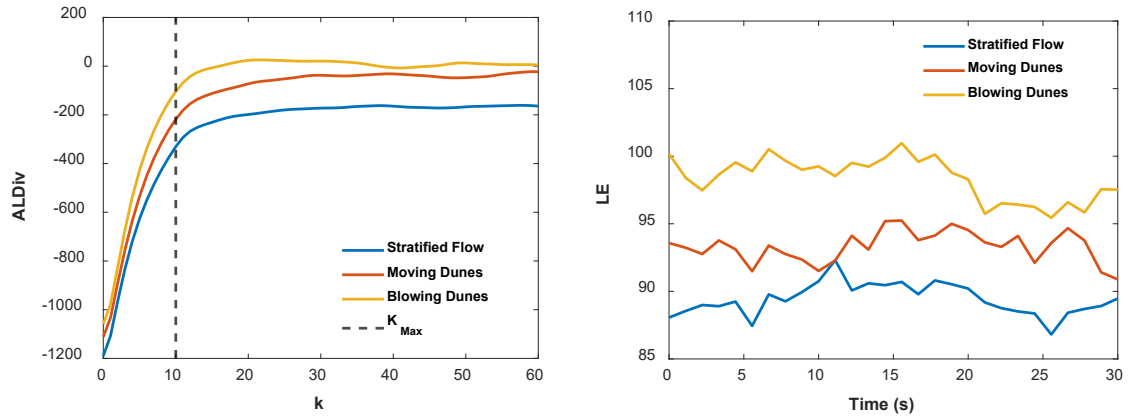

Figure 5 (a) An average log divergence vs expansion step and (b) LE time-series for bottom arc-shaped electrostatic sensor signals acquired at air velocities of 33, 20 and 10 m/s and solid mass flow rate of 3, 3.5 and 3.1 kg/s representing the stratified flow, moving dunes and blowing dunes respectively

Figure 6 shows the profile of the average LE over 30s data (15750 data points) across the operating points in the state diagram. The LE values have low correlations with the solids mass flow rates and high correlations with the air mass flow rates, making it a good observable candidate near the PMC even if the solids mass flow rate is unknown throughout the transport process. At constant solids mass flow rates and higher air velocities than the MCAV, the LE values have an inverse relationship with the air velocity and pressure drop. The relationship between the LE and pressure drop values changes to a direct relationship at air velocities below the MCAV, where the highest LE values are localised at the blowing dunes flow pattern left boundary.

In the stratified/pulsating flow region, the LE of electrostatic signals have relatively similar values, ranging between 87 to 99, indicating that the concentration of individual charged particles at the bottom of the pipeline in the stratified and pulsating flow have similar chaotic behaviour. However, a smooth transition in the LE values is present between the boundary separating stratified/pulsating flow from moving dunes to the left boundary of the blowing dunes region. This transition describes the increased chaotic behaviour of charged particles around dunes, where the dynamics of the electrostatic signal shift from the individual charged particles in suspension to creeping charged particles around dunes which increase in size with the decrease in air velocity.

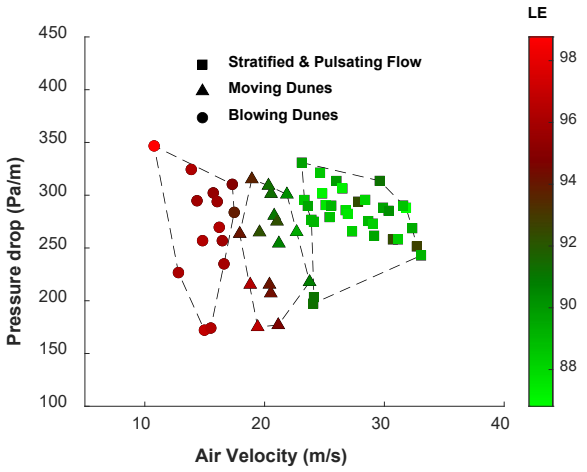

Figure 6 State diagram correlated with Lyapunov exponent of bottom arc-shaped electrostatic sensor signals

5. CONCLUSIONS

Chaos analysis is applied to bottom arc-shaped electrostatic signals in horizontal pneumatic conveying of plastic pellets to characterise the instability of gas-solid flow in the transition phase between dilute and dense phase conveying conditions. The optimal pneumatic transport operating conditions for minimum energy consumption is

at the PMC in a horizontal pneumatic conveying state diagram, located in the transition phase between dilute and dense phase conveying conditions. The state diagram of plastic pellets is developed using two operating parameters, air mass flow rate and solids mass flow rate, and correlated with the observed flow patterns, including stratified/pulsating flow, moving dunes, and blowing dunes. The PMC is found to be located between moving dunes and blowing dunes.

The largest Lyapunov exponent (LE) is a statistical measure describing the degree of chaos in time-series data, used to characterise the instabilities of electrostatic sensor time-series data in the transition phase conveying conditions. LE time series is calculated for phase spaces reconstructed from a moving window of electrostatic sensor data. The parameters used to calculate LE are set to constant values to have smooth values across time and be able to compare them at different pneumatic transport operating parameters. It is found that the LE time series values increase as the air velocity decrease for approximately constant solids mass flow rates ranging from 3 to 3.5 kg/s.

The average value of LE time-series across the 30s of electrostatic sensor data is correlated with the air velocity, pressure drop and observed flow patterns at various solids mass flow rates ranging from 2.2 to 4.2 kg/s. At constant air velocity, low correlation is found between LE and both solids mass flow rates and pressure drop. However, at constant solids mass flow rate and air velocity higher than the MCAV, the LE values have an inverse relationship with the air velocity and pressure drop. Below the MCAV, the LE values have an inverse relationship with the air velocity, which has a direct relationship with pressure drop.

6. ACKNOWLEDGEMENTS

The author would like to acknowledge the financial support from the University of Greenwich through VC scholarship (VCS-ES-04-19) and technical support from the entire team at the Wolfson Centre for Bulk Solids Handling Technology, University of Greenwich.

7. NOMENCLATURE

MCAV	Minimum conveying air velocity, m/s
PMC	Pressure drop minimum curve, Pa/m
P1 to P8	Pressure sensor tapings
t	Time, s
x(t)	Data point value at specific t
X(t)	Time series data
τ	Time delay
m	Embedding dimension
n	Number of data points
N	Number of phase points
Y(t)	Phase space (Time series vector)
i	Phase point index
s	Nearest neighbour phase point index
k	Expansion step
k_{Min}	Minimum expansion step
k_{Max}	Maximum expansion step
dt	Time difference between acquired data points
$\lambda(i)$	Lyapunov exponent
ALDiv	Average log divergence (mean of positive Lyapunov exponent across all dimensions)
LE	Largest Lyapunov exponent

8. REFERENCES

[1] P. W. Wypych and J. Yi, 'Minimum transport boundary for horizontal dense-phase pneumatic conveying of granular materials', *Powder Technol*, vol. 129, no. 1–3, pp. 111–121, 2003, doi: 10.1016/S0032-5910(02)00224-3.

[2] A. K. Saha, D. Das, R. Srivadtava, P. K. Panigrahi, and K. Muralidhar, *Fluid Mechanics and Fluid power - Contemporary Research*. 2016. doi: 10.1007/978-81-322-2743-4.

[3] A. B. Makwana, A. Patankar, and M. Bose, 'Effect of dune formation on pressure drop in horizontal pneumatic conveying system', *Particulate Science and Technology*, vol. 33, no. 1, pp. 59–66, 2015, doi: 10.1080/02726351.2014.936541.

[4] F. Takens, 'Detecting strange attractors in turbulence Dynamical Systems and Turbulence', *Dynamical Systems and Turbulence*, vol. 898, pp. 366–381, 1981, [Online]. Available: http://dx.doi.org/10.1007/bfb0091924

[5] Maiti and Bidinger, *Nonlinear Time Series Analysis*, Second edi. The press syndicate of the university of Cambridge, 2004.

[6] F. J. Cabrejos and G. E. Klinzing, 'Characterisation of dilute gas-solids flows using the rescaled range analysis', *Powder Technol*, vol. 84, no. 2, pp. 139–156, 1995, doi: 10.1016/0032-5910(95)02980-G.

[7] J. B. Pahk and G. E. Klinzing, 'Assessing flow regimes from pressure fluctuations in pneumatic conveying of polymer pellets', *Particulate Science and Technology*, vol. 26, no. 3, pp. 247–256, 2008, doi: 10.1080/02726350802028926.

[8] J. S. Shijo and N. Behera, 'Transient parameter analysis of pneumatic conveying of fine particles for predicting the change of mode of flow', *Particuology*, vol. 32, pp. 82–88, 2017, doi: 10.1016/j.partic.2016.07.004.

[9] H. Ji, H. Ohara, K. Kuramoto, A. Tsutsumi, K. Yoshida, and T. Hirama, 'Nonlinear dynamics of gas-solid circulating fluidised-bed system', *Chem Eng Sci*, vol. 55, no. 2, pp. 403–410, 2000, doi: 10.1016/S0009-2509(99)00335-8.

[10] N. Ellis, L. A. Briens, J. R. Grace, H. T. Bi, and C. J. Lim, 'Characterisation of dynamic behaviour in gas-solid turbulent fluidised bed using chaos and wavelet analyses', *Chemical Engineering Journal*, vol. 96, no. 1–3, pp. 105–116, 2003, doi: 10.1016/j.cej.2003.08.017.

[11] M. F. Llop, N. Jand, K. Gallucci, and F. X. Llauró, 'Characterising gas-solid fluidisation by nonlinear tools: Chaotic invariants and dynamic moments', *Chem Eng Sci*, vol. 71, pp. 252–263, 2012, doi: 10.1016/j.ces.2011.12.031.

[12] Y. Zhou, X. Zhu, and T. Qi, 'Fractal characteristic analysis of multi-source information of gas-solid two-phase flow in a riser', *Journal of Chemical Engineering of Japan*, vol. 50, no. 7, pp. 476–484, 2017, doi: 10.1252/jcej.16we203.

[13] Y. Lu *et al.*, 'Multi-scale characteristics and gas-solid interaction among multiple beds in a dual circulating fluidised bed reactor system', *Chemical Engineering Journal*, vol. 385, no. May 2019, 2020, doi: 10.1016/j.cej.2019.123715.

[14] F. Fu, M. Kong, C. Xu, C. Liang, and S. Wang, 'Flow characterisation of dense-phase pneumatic conveying system of pulverised coal through electrostatic sensor arrays', *Advances in Mechanical Engineering*, pp. 1–12, 2013, doi: 10.1155/2013/656194.

[15] A. Kumar, T. Deng, and M. S. A. Bradley, 'Application of arc-shaped electrostatic sensors for monitoring the flow behaviour at top and bottom section of a pneumatic conveying pipeline', *Measurement: Sensors*, vol. 10–12, no. 10–12, pp. 1–8, 2020, doi: 10.1016/j.measen.2020.100026.

[16] C. Rhodes and M. Morari, 'The false nearest neighbors algorithm: An overview', *Comput Chem Eng*, vol. 21, pp. 1149–1154, 1997, doi: 10.1016/S0098-1354(97)87657-0.

[17] M. T. Rosenstein, J. J. Collins, and C. J. de Luca, 'A practical method for calculating largest Lyapunov exponents from small data sets', *Physica D*, vol. 65, no. 1–2, pp. 117–134, 1993, doi: 10.1016/0167-2789(93)90009-P.

[18] M. G. Jones and K. C. Williams, 'Predicting the mode of flow in pneumatic conveying systems-A review', *Particuology*, vol. 6, no. 5, pp. 289–300, 2008, doi: 10.1016/j.partic.2008.05.003.

[19] Y. Tsuji, Y. Morikawa, S. Sugimotc, S. I. Miyoshi, and Y. Nakano, 'Flow Pattern and Pressure Fluctuation in Air-Solids Two-Phase Flow in a Pipe at Low Velocities', *International Journal of Multiphase Flow*, vol. 48, no. 428, pp. 656–663, 1982, doi: 10.1299/kikaib.48.656.